Patterned Growth of High-quality Single-walled Carbon Nanotubes from Dip-coated Catalyst

Rong Xiang, Erik Einarsson, Hiroto Okabe, Shohei Chiashi, Junichiro Shiomi, Shigeo Maruyama*

Department of Mechanical Engineering, The University of Tokyo

7-3-1 Hongo, Bunkyo-ku, Tokyo 113-8656, Japan

Abstract

Here we show that the conventional concept of using SiO_2 patterned Si substrates to selectively grow 3D carbon nanotube structures can also be applied to a dip-coating method. High-quality vertically aligned single-walled carbon nanotube (SWNT) patterns can be easily obtained by this protocol. Apart from the sintering of catalyst into Si at high temperature, the difference in surface wettability between Si and SiO_2 also plays an important role in this selective growth, which leads us to a novel method of patterning the growth on chemically modified surfaces.

KEYWORDS: SWNT, pattern, ACCVD, dip-coating, growth mechanism

1. Introduction

The excellent properties of carbon nanotubes (CNTs), particularly chirality-dependent electrical conductivity of single-walled carbon nanotubes (SWNTs), make them one of the most attractive building blocks for next-generation nano-devices.[1] Localizing the growth of SWNTs, therefore, has attracted much attention because it is a critical step in the fabrication of on-substrate devices.[2-5] Well patterned vertically aligned (VA-) CNTs have been used to construct field emission arrays,[6] super amphiphobic surfaces,[7] chip cooling microfins,[8] a dry 'gecko foot' adhesive,[9] a terahertz polarizer,[10] etc. The conventional way to pattern CNT growth involves selective sputtering (evaporation) of metal catalyst through a metal or photoresist mask.[6, 11, 12] Such dry catalyst deposition methods, although work well, require multiple steps and complicated facilities. A wet-based dip-coating approach possesses great advantages in cost and scalability.[13] However, conventional MEMS techniques such as lift-off are not compatible to this simple method in yielding patterned catalyst.

An alternative concept is to use the different growth behavior of CNTs on Si and SiO_2.[14] This method, however, has thus far only been successful in producing multi-walled CNTs by a ferrocene-based process. Here we borrow this concept and show that similar growth selectivity can also be obtained when dip-coating is used for catalyst preparation. SWNTs grow only in the SiO_2 regions of a Si and SiO_2 patterned substrate. The mechanism is not only due to the reaction between catalyst and Si at high temperatures, but also to the selective deposition of catalyst caused by the difference in surface wettability. This indicates that simply modulating the surface potential may also succeed in localizing catalyst deposition in wet-based dip-coating methods, and therefore localizing growth of SWNTs on a substrate.

2. Experimental

SWNT arrays were grown on SiO_2 patterned Si substrates using ethanol as a carbon source and Co as the catalyst.[15, 16] A 50 nm thick SiO_2 layer was patterned on a Si wafer using standard UV lithography combined with HF etching. A schematic showing the fabrication process is shown in Fig. 1a. The catalyst was loaded onto the substrate by the previously reported dip-coating process.[13, 17] The substrate was submerged into the dip-coating solution (0.1% wt. cobalt acetate in ethanol), soaked for 3 min, and withdrawn slowly at 4 cm/min. The substrate was then baked in air at 400 °C for 5 min before CVD. Only cobalt acetate was used here as the catalyst precursor because we recently found VA-SWNT arrays can still be obtained when Mo is absent, as long as the parameters are well optimized. ACCVD was performed at 700-800 °C with an ethanol flow of 450 sccm at a pressure of 1.3 kPa. The as-grown SWNTs were characterized using scanning electron microscopy (SEM, accelerated at 1 kV) and Raman spectroscopy (excitation laser wavelength 488 nm). Catalyst morphologies on the substrate surface were imaged by atomic force microscopy (AFM).

3. **Results and Discussion**

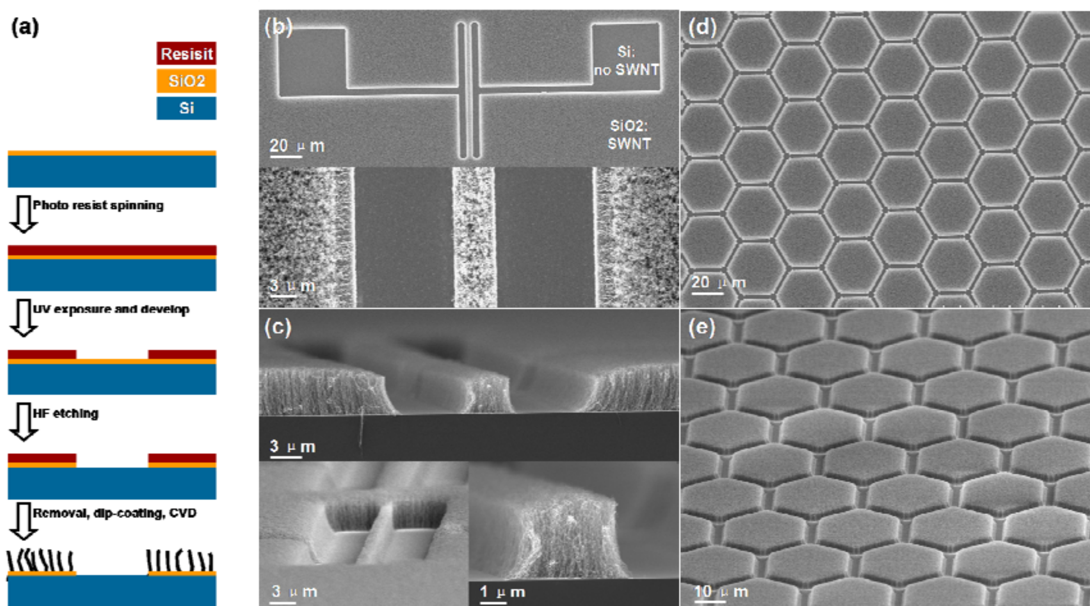

Figure 1

Figure 1(b) shows typical top-view SEM images of an electrode-shaped SWNT pattern. It is clear that SWNTs grow only in regions where an oxide layer is present. No growth was observed in areas where the oxide layer had been etched by HF. The SWNT structures can form lines, hexagons (Fig. 1d) or other shapes depending on the pre-designed pattern. The resolution of this method is limited by the ability of obtaining oxide area on a Si wafer. In this experiment, a linewidth of several micrometers was achieved using UV lithography. If other higher resolution techniques (e.g. electron-beam lithography, scanning probe oxidation) were used, finer SWNT structures may be obtained. The convenience in this approach is that the regions where SWNTs grow can be well controlled by pre-fabrication. Dip-coating was performed on the entire substrate and no further processing (e.g., lift–off) was needed.

The cross-sectional view of a pattern (Fig. 1c) confirmed the alignment of the obtained SWNTs. However, SWNTs can also grow into random networks if the catalyst density is significantly decreased. Both edges of a line pattern always exhibit transition regions, where the SWNTs are not perfectly perpendicular to the substrate. Apart from these few micrometers, however, the alignment is essentially the same as in VA-SWNT arrays. The formation of such transition regions is very likely due to the different wetting behavior of liquid at the edge (more discussion on this edge effect later). Further study is needed to understand and control this phenomenon.

Raman spectroscopy is a powerful tool to evaluate the existence and quality of SWNTs. Typical Raman spectra are presented in Fig. 2. For a pattern of SWNT stripes with the spacing larger than 10 micrometers, it is easy to focus the laser in the SWNT and non-SWNT areas, as shown in the inset optical microscope images. In the SiO_2 region, where SWNTs are expected to grow, strong and clear peaks are observed around 1592 cm^{-1} (G-band) and in the range from 100 to 300 cm^{-1} (radial breathing mode, RBM). A clear split of the G-band and

the strong intensity of RBM peaks confirm the existence of SWNTs. A weak D-band at 1344 cm^{-1} indicates that the SWNTs are well crystallized. In contrast, neither G-band nor RBM peaks were detected in the Si regions. This indicates there are essentially no SWNTs grown on Si, which is consistent with SEM observations. A sharp peak at 520 nm, attributed to bulk silicon, is observed in both Si and SiO_2 regions. It is also worth noting that, due to the strong resonance effect (particularly in the RBM region), Raman spectroscopy only provides information from a limited number of SWNTs in the entire array. Further characterization by transmission electron microscopy (TEM) revealed only SWNTs. The diameter range is from 1-3.5 nm, with a mean value slightly larger than 2 nm. When Co/Mo bimetal catalyst is used, however, the average diameter can be reduced.[17-19)]

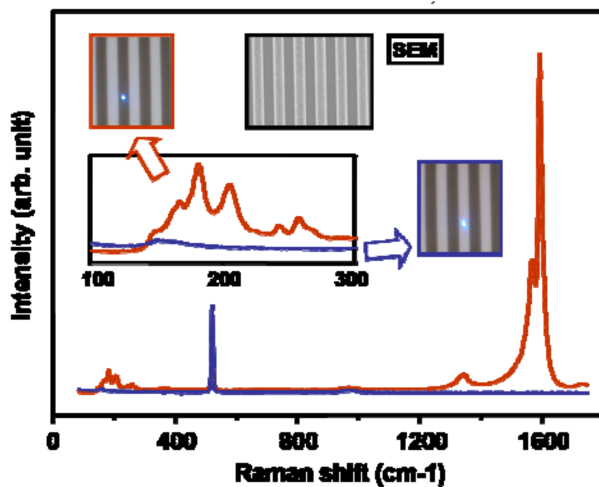

Figure 2

The growth selectivity of CNTs on Si and SiO_2 was believed to be due to the higher reactivity of metal with Si at high temperature. The sintering of Fe into a Si substrate at 800°C has also been directly observed by TEM.[20)] We believe such catalyst sintering will also happen in our process if the catalyst were uniformly deposited on both Si and SiO_2 surfaces. However, since dip-coating is a wet process, the difference in surface potential (i.e., wettability) may also play a critical role. SiO_2 is very hydrophilic, having a water contact angle of nearly 0°. Si, on

the other hand, is relatively hydrophobic, with a water contact angle of approximately 90°. This may also introduce some difference even in the dip-coating stage, meaning that catalyst may be selectively deposited on the oxide layer from the very beginning.

The difference in catalyst deposition is first evidenced by the temperature dependence of the selectivity between Si and SiO_2. Some reports have claimed that at lower temperature (e.g., 700°C), CNTs can also nucleate on a Si surface.[21, 22)] This is because the diffusion of metal into Si is considerably slowed. However, in our process no SWNTs were obtained at 700 or 750°C, which indicates that the reaction between metal and substrate may not be the dominant issue here.

Direct evidence was obtained by AFM imaging of the surface of Si and SiO_2 after catalyst preparation. Figure 3 shows the surface morphologies before and after CVD. In this case the catalyst density is low so that each particle can be clearly resolved. Interestingly, after calcination at 400°C, particles with diameter around 2 nm were already formed on the SiO_2 surface. On the Si surface, however, no particles were apparent. This confirms that clear differences exist even before reduction of catalyst at high temperature. Since oxide is not expected to react with the Si wafer, especially at only 400 °C, the difference should result directly from dip-coating. SEM images of the surface after CVD are consistent with AFM observations; the density of SWNTs grown after CVD is similar to that of the particles formed after calcination. No SWNTs were observed on Si.

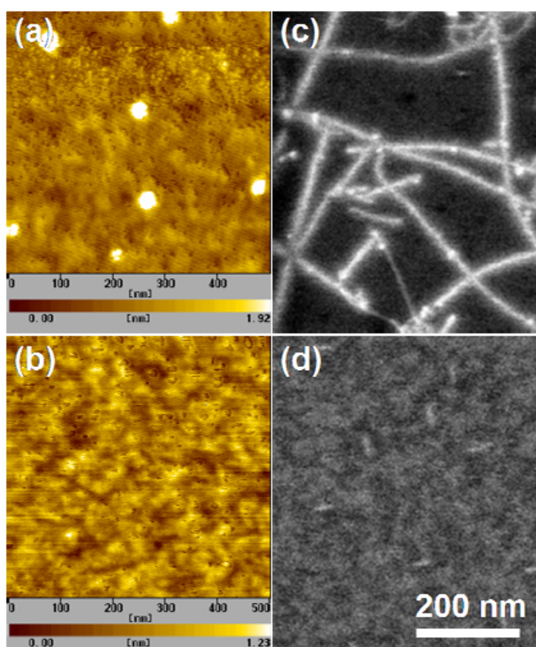

Figure 3

The surface-wettability induced selective deposition of catalyst is also supported by the edge shape seen in Fig. 1c. If there were no difference in wetting and drying of the catalyst solution between Si and SiO_2 catalyst particles would be expected to form uniformly on the entire surface, including the Si-SiO_2 boundary. In this case, the vertical alignment of the SWNT forest grown on a SiO_2 pattern should be perfect, i.e., no edge effect should be observed.

Finally, we propose some other strategies to tailor the surface wettability of SiO_2 to confirm its intrinsic effect on catalyst deposition by dip-coating. One effective approach to change SiO_2 from hydrophilic to hydrophobic is chemically modulating the termination group using a self-assembled monolayer (SAM). One advantage generated from this one-molecule-thick (~2 nm) covering is that the topography effect (which may affect the dip-coating when SiO_2 is 50 nm higher than Si) is minimized. Thus, if similar selective deposition of catalyst happens in such a system, the wettability difference between Si and SiO_2 must play an

important role. We found on SAM-functionalized surfaces, where the water contact angle is around 90°, the amount of SWNTs grown is considerably reduced. No growth occurs when the substrate is fully covered by SAM, even if the substrate is entirely SiO_2, thus changing only the surface wettability can also localize the SWNT growth to hydrophilic areas. Detailed experiments and discussion related to this topic has been reported separately.[23] Patterned growth of SWNTs on SiO_2 will be important for the realization of nanotube-based applications, such as field-effect transistors, where an oxide layer is needed as a back gate. For those applications demonstrated using multi-walled CNTs, as mentioned in the introduction, well patterned SWNTs may perform even better. Using liquid based dip-coating combined with ACCVD, large area high quality SWNT patterns can be produced at low cost.

4. Conclusions

We have shown that the classic concept of using SiO_2 patterned Si substrates to selectively grow 3D carbon nanotube structures can also be applied to a dip-coating method, and high-quality VA-SWNT patterns were obtained easily by this approach. The reason for the different SWNT growth behavior on Si and SiO_2 not only lies in the lower stability of catalyst on Si at high temperature, but also in the different wetting behavior during the dip-coating stage. This leads us to a novel method of patterning the growth on surface-modified substrates. This study broadens our understanding of liquid based dip-coating and provides us an alternative approach to fabricating 3D structures consisting of high-quality SWNTs.

References

1. Carbon Nanotubes: Advanced Topics in the Synthesis, Structure, Properties and Applications; Jorio, A., Dresselhaus, M. S., Dresselhaus, G., Eds.; Springer: 2007.
2. J. Kong, H. T. Soh, A. M. Cassell, C. F. Quate, H. J. Dai: Nature **395** (1998) 878.
3. S. M. Huang, L. M. Dai, A. W. H. MAU: Adv. Mater. **14** (2002) 1140.
4. A. Javey, H. J. Dai: J. Am. Chem. Soc. **127** (2005) 11942.
5. M. S. He, X. Ling, J. Zhang, Z. F. Liu: J. Phys. Chem. B **109** (2005) 10946.
6. S. S. Fan, M. G. Chapline, N. R. Franklin, T. W. Tombler, A. M. Cassell, H. J. Dai: Science **283** (1999) 512.
7. H. J. Li, X. B. Wang, Y. L. Song, Y. Q. Liu, Q. S. Li, L. Jiang, D. B. Zhu: *Angew. Chem.* Int. Ed. **40** (2001) 1743.
8. K. Kordás, G. Tóth, P. Moilanen, M. Kumpumäki, J. Vähäkangas, A. Uusimäki, R. Vajtai, P. M. Ajayan: Appl. Phys. Lett. **90** (2007) 123105.
9. L. Ge, S. Sethi, L. Ci, P. M. Ajayan, A. Dhinojwala: Proc. Natl. Acad. Sci. U.S.A. **104** (2007) 10792.
10. L. Ren, C. L. Pint, L. G. Booshenri, W. D. Rice, X. F. Wang, D. J. Hilton, K. Takeya, I. Kawayama, M. Tonouchi, R. H. Hauge, J. Kono: Nano Lett. **9** (2009) 2610.
11. K. Hata, D. N. Futaba, K. Mizuno, T. Namai, M. Yumura, S. Iijima: Science **306** (2004) 1362.
12. G. F. Zhong, T. Iwasaki, J. Robertson, H. Kawarada: J. Phys. Chem. B **111** (2007) 1907.
13. Y. Murakami, Y. Miyauchi, S. Chiashi, S. Maruyama: Chem. Phys. Lett. **377** (2003) 49.
14. B. Q. Wei, R. Vajtai, Y. Jung, J. Ward, R. Zhang, G. Ramanath, P. M. Ajayan: Nature **416** (2002) 495.
15. S. Maruyama, R. Kojima, Y. Miyauchi, S. Chiashi, M. Kohno: Chem. Phys. Lett. **360** (2002) 229.
16. Y. Murakami, S. Chiashi, Y. Miyauchi, M. H. Hu, M. Ogura, T. Okubo, S. Maruyama: Chem. Phys. Lett. **385** (2004) 298.
17. E. Einarsson, Y. Murakami, M. Kadowaki, S. Maruyama: Carbon **46** (2008) 923.
18. E. Einarsson, M. Kadowaki, K. Ogura, J. Okawa, R. Xiang, Z. Zhang, Y. Yamamoto, Y. Ikuhara, S. Maruyama: J. Nanosci. Nanotechnol. **8** (2008) 6093.
19. R. Xiang, Z. Yang, Q. Zhang, G. H. Luo, W. Z. Qian, F. Wei, M. Kadowaki, E. Einarsson, S. Maruyama: J. Phys. Chem. C **112** (2008) 4892.
20. Jung Y J, Wei B Q, Vajtai R, Ajayan P M, Homma Y, Prabhakaran K, Ogino T: Nano Lett. **3** (2003) 561.
21. Z. J. Zhang, Y. Zhou, Yue Y: Appl. Phys. Lett. **87** (2005) 223121.
22. R. Xiang, G. H. Luo, Z. Yang, Q. Zhang, W. Z. Qian, F. Wei: Nanotechnology **18** (2007) 415703.
23. R. Xiang, T. Z. Wu, E. Einarsson, Y. Suzuki, Y. Murakami, J. Shiomi, S. Maruyama: J. Am. Chem. Soc. **131** (2009) 10344.

Figure Captions

Figure 1: (a) Schematic showing the substrate fabrication and selective growth; (b) Top and (c) side view SEM images of an electrode-shaped pattern, where SWNTs only grew in the SiO_2 regions. (d) Top and (e) side view images of hexagon-shaped patterns. The growth behavior of SWNTs at the edges is slightly different from in the center of a vertically aligned forest.

Figure 2: Raman spectra from Si (blue) and SiO_2 (red) regions, showing that high-quality SWNTs are obtained on SiO_2 but almost no SWNTs grow on Si. The inset shows optical microscope and SEM images of linear SWNT patterns.

Figure 3: AFM images of (a) SiO_2 and (b) Si surfaces prior to CVD synthesis of SWNTs; SEM images of (c) SiO_2 and (d) Si surfaces after CVD. Catalyst deposition and SWNT growth occur on SiO_2 while growth on Si is considerably suppressed.